
Dynamic neural network modeling of thermal environments of two adjacent single-span greenhouses with different thermal curtain positions

Timothy Denen Akpenpuun, Qazeem Opeyemi Ogunlowo, Wook-Ho Na, Prabhat Dutta, Anis Rabiou, Misbaudeen Aderemi Adesanya, Mohammadreza Nariman, Ezatullah Zakir, Hyeon Tae Kim, Hyun-Woo Lee

Publisher's Disclaimer

E-publishing ahead of print is increasingly important for the rapid dissemination of science. The *Early Access* service lets users access peer-reviewed articles well before print/regular issue publication, significantly reducing the time it takes for critical findings to reach the research community.

These articles are searchable and citable by their DOI (Digital Object Identifier).

Our Journal is, therefore, e-publishing PDF files of an early version of manuscripts that undergone a regular peer review and have been accepted for publication, but have not been through the typesetting, pagination and proofreading processes, which may lead to differences between this version and the final one.

The final version of the manuscript will then appear on a regular issue of the journal.

Please cite this article as doi: 10.4081/jae.2024.1563

 ©The Author(s), 2024
Licensee [PAGEPress](#), Italy

Submitted: 04/02/2023

Accepted: 30/04/2023

Note: The publisher is not responsible for the content or functionality of any supporting information supplied by the authors. Any queries should be directed to the corresponding author for the article.

All claims expressed in this article are solely those of the authors and do not necessarily represent those of their affiliated organizations, or those of the publisher, the editors and the reviewers. Any product that may be evaluated in this article or claim that may be made by its manufacturer is not guaranteed or endorsed by the publisher.

Dynamic neural network modeling of thermal environments of two adjacent single-span greenhouses with different thermal curtain positions

Timothy Denen Akpenpuun,^{1,2} Qazeem Opeyemi Ogunlowo,^{3,4} Wook-Ho Na,² Prabhat Dutta,⁵ Anis Rabiou,³ Misbaudeen Aderemi Adesanya,³ Mohammadreza Nariman,⁶ Ezatullah Zakir,³ Hyeon Tae Kim,⁷ Hyun-Woo Lee^{2,3}

¹Department of Agricultural and Biosystems Engineering, University of Ilorin, Ilorin, Nigeria; ²Smart Agriculture Innovation Centre, Kyungpook National University, Daegu, Korea; ³Department of Agricultural Civil Engineering, College of Agricultural and Life Sciences, Kyungpook National University, Daegu, Korea; ⁴Department of Agricultural, and Bioenvironmental Engineering, Federal College of Agriculture, Moor Plantation, Ibadan, Nigeria; ⁵Department of Food Security and Agriculture Development, Kyungpook National University, Daegu, Korea; ⁶Department of Mechanics of Biosystem Engineering, Faculty of Engineering & Technology, College of Agriculture & Natural Resources, University of Tehran, Karaj, Alborz, Iran; ⁷Department of Bio-Systems Engineering, Institute of Smart Farm, Gyeongsang National University, Jinju, Korea;

Correspondence: Hyun-Woo Lee, Department of Agricultural Civil Engineering, College of Agricultural and Life Sciences, Kyungpook National University, Daegu 41566, Korea.

Tel.: +82.539505736.

E-mail: whlee@knu.ac.kr

Key words: neural network; NARX; modeling; time series; algorithm; normalization.

Contributions: TDA, WHN, HWL, conceptualization; HWL, TDA, WHN, QOO, MN, PD, AR, MAA, EZ, methodology; TDA, WHN, formal analysis; TDA, QOO, WHN, PD, AR, MAA, EZ, investigation; HWL, resources, project administration, funding acquisition; TDA, QOO, WHN, data curation; TDA, writing of original draft preparation; TDA, HTK, HWL, writing, review, and editing; TDA, WHN, visualization; HWL, HTK supervision. All authors read and approved the final version to be published.

Conflict of interest: the authors declare no potential conflict of interest.

Funding: this study was supported by the Korea Institute of Planning, and Evaluation for Technology in Food, Agriculture, Forestry, and Fisheries (IPET) through the Agriculture, Food, and Rural Affairs Convergence Technologies Program for Educating Creative Global Leaders, funded by the Ministry of Agriculture, Food, and Rural Affairs (MAFRA) (717001-7). This research was supported by the Basic Science Research Program through the National Research Foundation of Korea (NRF) funded by the Ministry of Education (NRF-2019R1I1A3A01051739).

Abstract

In order to produce marketable yield, scientific methodologies must be used to forecast the greenhouse microclimate, which is affected by the surrounding macroclimate and crop management techniques. The MATLAB tool NARX was used in this study to predict the strawberry yield, indoor air temperature, relative humidity, and vapor pressure deficit using input parameters such as indoor air temperature, relative humidity, solar radiation, indoor roof temperature, and indoor relative humidity. The data were normalized to improve the accuracy of the model, which was developed using the Levenberg–Marquardt backpropagation algorithm. The accuracy of the models was determined using various evaluation metrics, such as the coefficient of determination, mean square error, root mean square error, mean absolute deviation, and Nash–Sutcliffe efficiency coefficient. The results showed that the models had a high level of accuracy, with no significant difference between the experimental and predicted values. The VPD model was found to be the most important as it influences crop metabolic activities and its accuracy can be used as an indoor climate control parameter.

Introduction

A greenhouse is a structure with a transparent covering that creates a microclimate, which protects the crops grown within it from the external macroclimate (Zakir *et al.*, 2022). Controlled-environment agriculture or protected cultivation allows for the monitoring and maintenance of a desirable microclimate for each crop and makes it possible to grow crops in the off-season, increasing the crop yield and quality. Moreover, it enables the growth of crops in areas where the open-field macroclimate would normally not support their growth. In addition, protected cultivation offers greater predictability and reduces the cost of production (Russo *et al.*, 2014; Gorjian *et al.*, 2020; Akpenpuun *et al.*, 2022). Indoor agriculture or controlled-environment plant production system (CEPPS) has rapidly evolved from simple greenhouse structures to high-tech plant factories that can achieve optimal crop productivity and human labor utilization owing to recent advances in precision technology, data processing, and smart farming (Shamshiri *et al.*, 2018; Uyeh *et al.*, 2021b). Global challenges that greenhouse technology seeks to address include food scarcity fuel scarcity, natural resources scarcity, environmental pollution, and ecosystem instability (Kozai *et al.*, 1997; Akpenpuun *et al.*, 2020; Ogunlowo *et al.*, 2022). When compared to open-field cultivation, protected cultivation techniques typically have higher returns per unit area. Because of the non-static conditions of the macroclimate, installed microclimate monitoring and control equipment and crop production systems are complex and dynamic (Azaza *et al.*, 2015; Uyeh *et al.*, 2021a). Greenhouse systems can be found all over the world with a variety of climatic conditions.

Therefore, to achieve favorable environmental conditions for plant growth, these production systems must be designed in such a way that the various components, shapes, glazing material, shading materials, and indoor operations are based on prevalent production systems site conditions. As a result of their importance in food safety and security, these systems have recently received a lot of attention (Fitz-Rodríguez *et al.*, 2010; Hu *et al.*, 2011; Su *et al.*, 2017; Escamilla-García *et al.*, 2020; Uyeh *et al.*, 2021a; Rabiou *et al.*, 2022). Because of the complexity of protected farming systems and variety of crops that can be grown in them, the general rule is to focus on factors that are most important for plant growth (Escamilla-García *et al.*, 2020).

A machine learning algorithm based on the concept of human neurons is known as artificial neural network (ANN). ANNs are a popular forecasting model that have been successful in forecasting process in many fields. ANNs are valuable and appealing for forecasting tasks due to several distinguishing characteristics, such as being data-driven, self-adaptive, having the potential to be generalized, and having the ability to learn the sample data and infer correctly even with noisy data (Taki *et al.*, 2016). Moreover, ANNs can work as universal functional estimators. It has been demonstrated that a network can approximate any continuous function to any desired accuracy. In addition, ANNs are capable of solving both linear and nonlinear problems (Khashei *et al.*, 2010). Since the development of effective neural network training tools to successfully model microclimate and yield prediction, several researchers have used neural networks (NN) to model nonlinear relationships governing the greenhouse environment (Zeng *et al.*, 2012; Taki *et al.*, 2016; Owolabi *et al.*, 2017; Singh *et al.*, 2017; Hongkang *et al.*, 2018). Moon *et al.* (2018), for example, developed an ANN prediction model to predict CO₂ concentration using temperature, relative humidity (RH), atmospheric pressure, and solar radiation as input. They established that ANN accurately estimated CO₂ concentration in the greenhouse with an accuracy of 97%. NNs models have been demonstrated to be reliable, suitable for modeling dynamic systems in real-time, and capable of solving nonlinear system relationships that are difficult to solve using traditional modeling techniques. However, none of the models took into account vapor pressure deficit (VPD), another important climate parameter, and the majority of these researchers used the feedforward neural network (FFNN) with daily or hourly mean data, which was often very short, ranging from 14 to 60 days. Furthermore, because the previously developed ANN models are specific to greenhouse types and locations, they cannot be used for new greenhouses in new locations because the models lack explicit structural components and other parameters in common.

In response to the knowledge gap identified in the literature, predictive models for indoor climate parameters were developed for two single-span gothic greenhouses. Because greenhouse microclimates are complex, multiparametric, nonlinear, and their climates are influenced by

macroclimate conditions, planted crops, structural members, accessories, and equipment, the dynamic feedback time series nonlinear autoregressive external (Exogenous) input (NARX) neural network was used in this study. NARX models are a type of nonlinear recurrent neural network that can be used to model dynamic systems with inputs and outputs that are time series data. They are particularly useful for predicting time series data when there is a nonlinear relationship between the inputs and outputs, and when there are exogenous inputs (inputs that are not part of the system being modeled). The Levenberg–Marquardt backpropagation algorithm was used to train, validate, and test the network using data collected from the two greenhouses over six months because the algorithm gave the best model evaluating parameter in terms of mean square error (MSE) and coefficient of determination (R^2). The models were further evaluated using root mean square error (RMSE), mean absolute deviation (MAD), and Nash–Sutcliffe efficiency coefficient (NSE). This research was carried out using data collected from two single-span double-layer greenhouses that had different thermal curtain positions (R greenhouse (RGH) had its thermal curtain located directly at the roof ridge, while the Q greenhouse (QGH) had its thermal screen at 5 degrees from the centre of the roof ridge). This was done to determine the effect of the thermal curtain position on the microclimate of the greenhouses.

Materials and Methods

Experimental setup and data acquisition

The experiments were performed in two greenhouses (RGH and QGH) on the Smart Agricultural Innovation Centre's greenhouse farm at 35.89°N and 128.61°E coordinates in Daegu, Republic of Korea. The greenhouses (oriented in the east-west) had the same structural configurations (gothic roofed), polyethylene glazing (thickness: 150 μm ; transmittance: 91%), motorized thermal screen (thermal conductivity ($0.037 \text{ Wm}^{-1}\text{K}^{-1}$), thermal radiation transmittance ($<0.001\%$), reflectance (0.10), and emittance (0.90)), roof and side vents, dimensions ($22 \text{ m} \times 8.4 \text{ m} \times 4 \text{ m}$), and four 0.5 hp air-circulating fans. The motorized roof and side vents were activated at 21°C and 23 °C, respectively, while the boiler activation and deactivation temperature range were 7.5°C–8.5°C as 8°C is the minimum temperature recommended for optimum strawberry growth and development. The primary fuel source for the boiler to generate heat was diesel fuel. The boilers' heating range was 15,000 kcal/h to 62,802 kcal/h, while the heating efficiency and continuous hot water supply were both 90% each. The same open-loop fertigation system was activated five times daily at 90 minutes intervals beginning at 0830 for a 3 minutes fertigation period. Solar radiation, RH, and air temperature were the environmental parameters measured in both greenhouses, and these were measured using standard sensing devices. The five-month experiments were conducted from November 2021 to April 2022.

Figures 1, 2 and 3 show a greenhouse model, experimental greenhouses showing thermal screen positions and sensor positions in both greenhouses.

The Seolhyang strawberry cultivar was planted in 76 cm wide and 1500 cm long greenhouse beds, with 30 cm spacing between plants on each bed. Each greenhouse bed was divided into five plots for a total of 25 plots. Standard strawberry cultivation practices are being implemented. Fruits were harvested from December 2021 to April 2022 and only marketable fruits (diameter > 20 mm; weight > 5 g) were used for analysis. The air temperature and RH sensors (temperature measurement range -20°C to 80°C , accuracy of $\pm 0.25^{\circ}\text{C}$; humidity measurement range of 0% to 100%, accuracy of $\pm 2\%$, HOBO PRO v2 U23 Pro v2, ONSET, USA) were installed (three per row) at 1.54 m from the floor and placed in protective plastic cases to shield them from direct solar radiation, which could lead to data inaccuracies. The solar radiation sensors (HOBO RX3000, ONSET, USA, measurement range: 0 to 1280 W/m^2 ; accuracy: $\pm 10 \text{ W/m}^2$ operating temperature range: -40°C to 70°C) were installed just above the crop canopy. All data loggers recorded readings every ten minutes. The vapor pressure deficit (VPD) was computed using the following equations 1-4 (Abd-El Baky *et al.*, 2004).

$$VP_{\text{sat}} = \exp^{(Z)} \quad (1)$$

$$Z = \frac{A}{T} + B + C(T) + DT^2 + ET^3 + F \ln T \quad (2)$$

$$VP_{\text{air}} = \frac{VP_{\text{sat}} \times RH}{100} \quad (3)$$

$$VPD = (VP_{\text{sat}} - VP_{\text{air}}) \frac{145}{1000} \quad (4)$$

where:

$$A = -1.044 \times 10^4; B = -1.129 \times 10^1; C = -2.702 \times 10^{-2}$$

$$D = +1.289 \times 10^{-5}; E = -2.478 \times 10^{-9}; F = + 6.545$$

T = air temperature in $^{\circ}\text{C}$; RH = air relative humidity (%) of the greenhouse

VP_{sat} = air saturation vapor pressure (psi); VP_{air} = vapor pressure of the air (psi)

VPD = vapor pressure deficit (kPa)

The yield data was prepared using the resampling technique. Data resampling involves the upsampling or downsampling technique. Upsampling technique was, however, used in this study to adjust the frequency of the yield data to match the climate data. The upsampling techniques is shown in equation 5.

$$y[n] = x\left[\frac{n}{L}\right], \text{ for } n = 0, 1, 2, \dots, (L - 1)N \quad (5)$$

where $x[n]$ is the original discrete time signal, L is the upsampling factor, and $y[n]$ is the upsampled signal. The length of the upsampled signal is L times the length of the original signal.

The data was normalized in MATLAB using the minimum–maximum normalization method to address the issue of differences in units and orders of magnitude between the input and target variables, as shown in equation 6.

$$x' = \frac{x_i - x_{\min}}{x_{\max} - x_{\min}} \quad (6)$$

x' = normalized or standardized value/score; x_i = raw individual data; x_{\min} = population minimum value; x_{\max} = population maximum value

Description of the network

A neural network algorithm for the indoor climate of two gothic greenhouses was proposed. To begin, the coefficient of determination (R^2) was used in Matrix Laboratory to select the best network training algorithm from Levenberg–Marquardt (LM), Bayesian regularization BR), and scaled conjugate gradient of the NARX dynamic multi-layer perceptron ANN time series methodology (MATLAB version R2021a, MathWorks, Inc, USA). To have a seamless network architecture, and model the following was done: the

- (a) nine predictor inputs (indoor air temperature, RH, VPD, indoor roof temperature (irT), indoor roof relative humidity (irRH), and solar radiation, and outside temperature RH, and SR).
- (b) nine inputs for predicting indoor RH (indoor air temperature, RH, VPD, indoor roof temperature (irT), indoor roof relative humidity (irRH), and solar radiation, and outside temperature RH, and SR).
- (c) nine predictor inputs (indoor air temperature, RH, VPD, indoor roof temperature (irT), indoor roof relative humidity (irRH), and solar radiation, and outside temperature, RH, and SR).
- (d) the data was divided into three subsets: training, testing, and validation and the target timesteps were 70%, 15%, and 15%.
- (e) the network architecture (Figure 1) was trained by varying the number of input/feedback delays while keeping the number of hidden neurons constant. The training process was iterated until the model with the best validation matrices (R^2 , RMSE, MAD MAPE), and Nash-Sutcliffe efficiency coefficient (NS)) were obtained. To determine the ideal number of neurons in the hidden layer, the rule of thumb that states the number of hidden neurons should be between the size of the input layer and the size of the output layer was used in this work. Based on this rule of thumb, four hidden layers of neurons were used to avoid overfitting or underfitting.
- (f) the best model selected from step (e) was chosen, and the predicted climate parameters were retrieved and analyzed.

Figures 4 and 5 show the NARX architecture and MATLAB NARX neural network diagram. The Nonlinear AutoRegressive model with eXogenous inputs (NARX) is an architecture used in dynamic

artificial neural networks (ANNs). The NARX architecture is designed to capture the relationship between an input sequence (the exogenous input) and an output sequence (the endogenous input) that may have a time lag. The NARX model has a feedforward structure that consists of a series of input layers, hidden layers, and output layers.

Statistical analysis

The observed and predicted data were compared to see if they differed significantly from each other. The null hypothesis assumed that the observed and predicted data samples were identical, whereas the alternative hypothesis assumed that the data sets were not identical. These hypotheses were tested using a confidence level of 95% (p -value = 0.05).

The coefficient of determination (R^2), which is a measure of the correlation between the observed and predicted values, the MSE, the RMSE, the MAD, and the Nash–Sutcliffe efficiency coefficient (NSE) of the developed model were determined using equations 7–10. The RMSE can be used to calculate the degree of dispersion of a prediction against the measured, and the MAD can be used to calculate the model's tendency for overestimation or underestimation. Low values of MAD, MSE, and RMSE are desired for good model accuracy. The Nash–Sutcliffe efficiency coefficient is used to describe the accuracy of model output with observed data. An NSE value of 1 represents a perfect match between observed data and outputs. As a result, the closer the model efficiency is to unity, the more accurate the model is (Adesanya *et al.*, 2022).

$$\text{MSE} = \frac{\sum(\beta_{\text{predicted}} - \beta_{\text{actual}})^2}{\text{nobs}} \quad (7)$$

$$\text{RMSE} = \sqrt{\text{MSE}} \quad (8)$$

$$\text{MAD} = \frac{1}{n} \sum_{t=1}^n \left| \frac{\beta_{\text{actual}} - \beta_{\text{predicted}}}{\text{nobs}} \right| \quad (9)$$

$$\text{NSE} = 1 - \frac{\sum(\beta_{\text{predicted}} - \beta_{\text{actual}})^2}{\sum(\beta_{\text{actual}} - \bar{m}_{\text{actual}})^2} \quad (10)$$

$\beta_{\text{predicted}}$ = predicted data; β_{actual} = experimental data; \bar{m}_{actual} = mean experimental data; nobs = number of observations; \bar{m} = mean of experimental data

Results

The data collected from two greenhouses, referred to as RGH and QGH, is presented in Table 1. The statistics indicate that the RGH had a higher average temperature and vapor pressure deficit compared to the QGH. However, the QGH had a higher relative humidity. Both greenhouses had similar mean solar radiation values. The RGH had a mean temperature of 20.01 ± 4.78 °C and a mean VPD of

1.23±0.86 kPa, while the QGH had a mean relative humidity of 52.36±2.06%. The mean SR for the RGH and QGH were 254±150.67 Wm⁻² and 205±127.64 Wm⁻² respectively.

To predict, a NARX neural network was utilized with indoor temperature, relative humidity, vapor pressure deficit, solar radiation, roof temperature, roof relative humidity, outside temperature, and outside relative humidity as inputs. The network was trained, validated, and tested using a ratio of 70:15:15, with 10 hidden neurons and 2, 3 and 4 delays.

The NARX neural network was trained, validated, and tested using indoor air temperature, RH and VPD as the target variables and the indoor air temperature, RH, VPD, SR, irT and irRH, and outdoor temperature, RH and SR as the inputs. The result of the process is presented in Tables 2 and 3. In most cases, the 70:15:15 training, validation, and testing ratio with 10 number of hidden neurons and 4 delays resulted in higher R-squared values and low MSE, RMSE, and MAD.

The analysis of variance (ANOVA) presented in table 4 shows that the actual and predicted were statistically insignificantly at the 95% confidence level. The ANOVA revealed that the actual and predicted values were not significantly different at both the 95% and 99% confidence levels (df1 = 1; df2 = 8110), which is desirable. There was no significant difference between the actual and predicted yield within the same greenhouse whereas there was a significant difference between the actual and predicted yield among the greenhouses with the QGH having higher yield. The MAD and NSE were 0.01 and 1.00 in both greenhouses. This means that the NARX model used to make predictions was able to accurately represent the actual values, as the difference between the two was not statistically significant. This implies that the model is reliable and can be used for future predictions with a high level of confidence. Figures 6 to 8 show the trend of the predicted parameters in RGH vs QGH.

Table 5 shows the predicted mean indoor air temperature, relative humidity (RH), vapor pressure deficit (VPD) and yield for RGH and QGH. The predicted mean of indoor air temperature, RH, VPD and yield for the RGH is 20.1±4.64 °C, 50.35±21.17%, 1.31±0.63 kPa and 6.33±1.58 g, respectively, while for the QGH it is 19.29±4.69 °C, 52.33±20.56%, 1.21±0.76 kPa and 7.72±1.92 g, respectively. The MAD for temperature, RH, VPD and yield for RGH is 1.96 °C, 8.58%, 0.28 kPa and 0.01, respectively and for QGH it is 2.10 °C, 7.58%, 0.24 kPa and 0.01, respectively. The Analysis of variance performed on the predicted VPD in the RGH and QGH at 5% level of confidence showed that there was a significant difference between the VPD in both greenhouses.

The MAD of all the predicted parameters was less than the mean of each predicted indoor parameters and yield. This result meets the requirement that a MAD value less than or equal to the dataset means is desirable and considered a good result. A low MAD indicates that the majority of the data values are close to the mean (since the expected distance from each data value to the mean is small). A large MAD indicated that many of the data values are far from the mean. The Nash–Sutcliffe efficiency

coefficient, also known as the sensitivity coefficient, was 0.68, 0.68, 0.78 and 1.00, and 0.65, 0.73, 0.82 and 1.00 for indoor air temperature, Rh, VPD and yield, respectively. These NSE values indicate that the accuracy of modeled outputs concerning observed data depicts a perfect match, as the closer the model efficiency is to unity, the more accurate the model.

Table 6 depicts the frequency distribution of VPD in the RGH and QGH. The QGH had higher percentages of VPD within the optimal band than the RGH and lower VPD percentages outside the optimal band.

Discussion

The NARX models were evaluated to determine prediction accuracy in terms of MSE, RMSE, MAD, and NS. Although indoor air temperature, RH, and VPD were modeled in this study, only the VPD was used later to evaluate the thermal environment of the greenhouses and compare the NARX models because VPD is the primary parameter that controls most of the plant metabolic activities, such as transpiration and photosynthesis rates, evaporation from plant leaves, and stomatal opening, which controls carbon dioxide assimilation, and nutrients and water uptake. In two greenhouses adjacent to each other, the NARX neural network was used to train, validate, and test the network for indoor air temperature, RH, and VPD. The NARX VPD model showed that the highest R^2 in the RGH was 99.1%, 98.7% and 98.6% for the 70:15:15 network architecture and 10:4 neuron-delays ratios. The corresponding validation MSE and RMSE value of 1.04×10^{-4} and 1.02×10^{-4} , and MAD, and NS value were 0.28, and 0.78, respectively, in the RGH. The NARX model for the QGH showed that the model was good in terms of training R^2 , training MSE, and RMSE, MAD and NS values of 98.9%, 8.66×10^{-4} , and 2.94×10^{-4} , 0.24 and 0.78, respectively. These models have satisfied the conditions of MSE, RMSE, and NSE, therefore, they are considered to be good based on these model evaluating parameters. Seginer *et al.* (1994) predicted greenhouse climate using a fitting NN model tool trained with experimental data from two greenhouses in Avignon, France, and Silsoe, UK, and obtained R^2 values of 0.95 for Avignon, and 0.97 for Silsoe. To characterize the indoor air temperature of a naturally ventilated greenhouse in Western Europe using outside air temperature and RH, global solar radiation received, and the amount of cloud cover, Frausto *et al.* (2003) also developed a linear autoregressive model with external input (ARX) and autoregressive moving average models with external input (ARMAX). They obtained R^2 ranges of 0.85 to 0.99 for ARMAX and 0.93 to 0.99 for ARX models. However, due to a lack of adaptability to extended periods and the low accuracy of these models compared to NARX. Frausto *et al.* (2004), on the other hand, created an autoregressive moving average model with external input (NNARX) model by combining linear autoregressive models (ARX) with neural network architectures and predicted internal greenhouse temperature as a

function of outside air temperature and humidity, global solar radiation, and sky cloudiness with corresponding goodness of fit of 75%, which is lower than the lowest goodness of fit of 96.8% obtained using. This shows that NARX has a higher predicting accuracy than other neural network tools. Dariouchy *et al.* (2009), on the other hand, obtained 0.987 and 0.972, and 0.991 and 0.989 for training temperature and humidity, respectively, while using a neural network fitting tool to predict internal temperature and humidity while using a neural network fitting tool to predict the internal temperature and humidity in a greenhouse with external humidity, total radiation, wind direction, wind speed, and temperature as inputs in a 7 days experiment. Similarly, Taki *et al.* (2016) predicted inside roof temperature (T_{ri}), indoor air humidity (RH_{is}), soil temperature (T_{is}), and soil humidity (RH_{ia}) of a semi-solar greenhouse using roof temperature, inside air humidity, soil temperature, inside radiation, and inside air temperature as inputs. Taki *et al.* (2016) found 0.25°C , 0.30%, 1.06°C , and 0.25% for T_{ri} , RH_{is} , T_{is} , and RH_{ia} , and concluded that ANN is a promising tool for predicting indoor climate and is useful in fully automated greenhouses. Petrakis *et al.* (2022) nonlinear designed a to model the internal temperature, RH, wind speed, and solar irradiance of a greenhouse using the Levenberg–Marquardt training algorithm with external temperature, RH, wind speed, and solar irradiance as input variables, and internal temperature, and RH as output/target variables. Petrakis *et al.* (2022) reported an R^2 of 99.9% for internal temperature and RH. Even though Petrakis *et al.* (2022) obtained an R^2 close to 100%, the accuracy of the nonlinear input–output neural network cannot be compared to the nonlinear autoregressive with external (Exogenous) input (NARX) used in this study. The use of nonlinear autoregressive with external (Exogenous) input (NARX), dynamic NN, and one of the neural network time series applications has demonstrated that it is the best predicting tool. Indoor microclimate revealed that the position of the thermal curtain had a significant influence on the VPD, which is considered the most important indoor climate parameter.

Conclusions

Greenhouse microclimate modeling is important because the microclimate is a dynamic system that is considerably influenced by the macroclimate of the surroundings, thereby making its modeling by conventional methods and techniques difficult. Therefore, the advent of the dynamic artificial neural networks (ANN) through Nonlinear AutoRegressive models with eXogenous inputs (NARX) modeling tool in MATLAB has enabled the modeling of dynamics and complex systems, such as the greenhouse microclimate, with high accuracy and reliability as compared to the general ANN models. The NARX modeling tool was able to reliably model the nonlinear and dynamic greenhouse environment of two gothic greenhouses with various thermal curtain positions, and the results obtained using such models like this can aid in the design of control systems based on the VPD, which

is a climate parameter that more accurately describes the environment than temperature and RH. Thus, this study shows that using a dynamic neural network model to simulate the thermal environments of greenhouses with different thermal curtain positions is effective. The comparison of the VPD in the RGH and QGH showed that the RGH had 36.1% of its VPD readings within the optimal range of 0.5-1.19 kPa, whereas the QGH had 46% of VPD data within the optimal range. There was also a significant difference ($p < 0.05$) between the VPD recorded in the two greenhouses with the QGH having better VPD readings than the RGH. This model can be used to optimize the thermal environment of greenhouses and improve the growth and productivity of plants. The dynamic ANN model was preferred over the general ANN model because the dynamic ANN models is capable of nonlinear modeling, can model the time-dependent relationship between variables, high accuracy, enhanced predicting capabilities and good adaptation to change. Despite the advantages of using the dynamic ANN models through NARX the following challenges might be encountered in its implementation (1) complex model design is required, (2) significant amount of data is required to accurately capture the complex and nonlinear relationships between the variables, and (3) require high computational resources. The potential use of dynamic ANN models can help to understand the impact of reducing greenhouse gas emissions or increasing the use of renewable energy sources and can also help in identifying feedback loops that amplify the impact of climate change.

References

- Abd-El Baky, H. M., Ali, S. A., El Haddad, Z. A., El Ansary, M. Y. 2004. Some Environmental Parameters Affecting Sweet Pepper Growth and Productivity Under Different Greenhouse Forms in Hot and Humid Climatic Conditions. *Mansoura University Journal of Soil Sciences and Agricultural Engineering*. 1:225-47.
- Adesanya, M. A., Na, W.-H., Rabi, A., Ogunlowo, Q. O., Akpenpuun, T. D., Rasheed, A., Yoon, Y. C., Lee, H.-W. 2022. TRNSYS Simulation and Experimental Validation of Internal Temperature and Heating Demand in a Glass Greenhouse. *Sustainability*. 14:8286.
- Akpenpuun, T. D., Mijinyawa, Y. 2020. Impact of a split-gable greenhouse microclimate on the yield of irish potato (*solanum tuberosum* l.) under tropical conditions. *Journal of Agricultural Engineering and Technology*. 25:54-78.
- Akpenpuun, T. D., Ogunlowo, Q. O., Rabi, A., Adesanya, M. A., Na, W. H., Omobowale, M. O., Mijinyawa, Y., Lee, H. W. 2022. Building energy simulation model application to greenhouse microclimate, covering material and thermal blanket modelling: A Review. *Nigerian Journal of Technological Development*. 19:276-86.

- Azaza, M., Echaieb, K., Tadeo, F., Fabrizio, E., Iqbal, A., Mami, A. 2015. Fuzzy decoupling control of greenhouse climate. *Arabian Journal for Science and Engineering*. 40:2805-12.
- Dariouchy, A., Aassif, E., Lekouch, K., Bouirden, L., Maze, G. 2009. Prediction of the intern parameters tomato greenhouse in a semi-arid area using a time-series model of artificial neural networks. *Measurement*. 42:456-63.
- Escamilla-García, A., Soto-Zarazúa, G. M., Toledano-Ayala, M., Rivas-Araiza, E., Gastélum-Barrios, A. 2020. Applications of artificial neural networks in greenhouse technology and overview for smart agriculture development. *Applied Sciences*. 10:3835.
- Fitz-Rodríguez, E., Kubota, C., Giacomelli, G. A., Tignor, M. E., Wilson, S. B., McMahon, M. 2010. Dynamic modeling and simulation of greenhouse environments under several scenarios: A web-based application. *Computers and Electronics in Agriculture*. 70:105-16.
- Frausto, H. U., Pieters, J. G. 2004. Modelling greenhouse temperature using system identification by means of neural networks. *Neurocomputing*. 56:423-28.
- Frausto, H. U., Pieters, J. G., Deltour, J. M. 2003. Modelling greenhouse temperature by means of auto regressive models. *Biosystems Engineering*. 84:147-57.
- Gorjian, S., Calise, F., Kant, K., Ahamed, M. S., Copertaro, B., Najafi, G., Zhang, X., Aghaei, M., Shamshiri, R. R. 2020. A review on opportunities for implementation of solar energy technologies in agricultural greenhouses. *Journal of Cleaner Production*. 285:124807.
- Hongkang, W., Li, L., Yong, W., Fanjia, M., Haihua, W., Sigrimis, N. A. 2018. Recurrent neural network model for prediction of microclimate in solar greenhouse. *IFAC-PapersOnLine*. 51:790-95.
- Hu, H.-G., Xu, L.-H., Wei, R.-H., Zhu, B.-K. 2011. RBF Network Based Nonlinear Model Reference Adaptive PD Controller Design for Greenhouse Climate. *International Journal of Advancements in Computing Technology*. 3:357-66.
- Khashei, M., Bijari, M. 2010. An artificial neural network (p, d, q) model for time series forecasting. *Expert Systems with Applications*. 37:479 – 89.
- Kozai, T., Kubota, C., Kitaya, Y. (1997, Aug. 26-29, 1996). Greenhouse technology for saving the earth in the 21st century. Paper presented at the Plant production in closed ecosystems (Proc. Intl. Symp. on plant production in closed ecosystems), Narita, Japan.
- Ogunlowo, Q. O., Na, W. H., Rabi, A., Adesanya, M. A., Akpenpuun, T. D., Kim, H. T., Lee, H. W. 2022. Effect of envelope characteristics on the accuracy of discretized TRNSYS building energy simulation model. *Journal of Agricultural Engineering*. 53:1420.

- Owolabi, A. B., Lee, J. W., Jayasekara, S. N., Lee, H. W. 2017. Predicting the Greenhouse Air Humidity Using Artificial Neural Network Model Based on Principal Components Analysis. *Journal of the Korean Society of Agricultural Engineers*. 59:93-99.
- Petrakis, T., Kavga, A., Thomopoulos, V., Argiriou, A. A. 2022. Neural Network Model for Greenhouse Microclimate Predictions. *Agriculture*. 12:780.
- Rabiu, A., Na, W., Akpenpuun, T. D., Rasheed, A., Adesanya, M. A., Ogunlowo, Q. O., Kim, H. T., Lee, H.-W. 2022. Determination of overall heat transfer coefficient of greenhouse energy-saving screens using TRNSYS and hotbox methods. *Biosystems Engineering*. 217:83-101.
- Russo, G., Anifantis, A. S., Verdiani, G., Mugnozza, G. S. 2014. Environmental analysis of geothermal heat pump and LPG greenhouse heating systems. *Biosystems Engineering*. 127:11-23.
- Seginer, I., Boulard, T., B.J. Bailey 1994. Neural network models of the greenhouse climate. *Journal of Agricultural Engineering Research*. 59:203-16.
- Shamshiri, R. R., Kalantari, F., Ting, K. C., Thorp, K. R., Hameed, I. A., Weltzien, C., Ahmad, D., Shad, Z. M. 2018. Advances in greenhouse automation and controlled environment agriculture: A transition to plant factories and urban agriculture. *International Journal of Agricultural and Biological Engineering*. 11:1-22.
- Singh, V. K., Tiwari, K. N. 2017. Prediction of greenhouse micro-climate using artificial neural network. *Applied Ecology and Environmental Research*. 15:767 - 78.
- Su, Y., Xu, L. 2017. Towards discrete time model for greenhouse climate control. *Engineering in Agriculture, Environment and Food*. 10:157 - 70.
- Taki, M., Ajabshirchi, Y., Ranjbar, S. F., Matloobi, M. 2016. Application of Neural Networks and multiple regression models in greenhouse climate estimation. *Agricultural Engineering International: CIGR Journal*. 18:29 - 43.
- Uyeh, D. D., Basse, B. I., Mallipeddi, R., Asem-Hiablie, S., Amaizu, M., Woo, S., Ha, Y. 2021a. A reinforcement learning approach for optimal placement of sensors in protected cultivation systems. *IEEE Access*. 9:100781-800.
- Uyeh, D. D., Pamulapati, T., Mallipeddi, R., Park, T., Woo, S., Lee, S., Lee, J., Ha, Y. 2021b. An evolutionary approach to robot scheduling in protected cultivation systems for uninterrupted and maximization of working time. *Computers and Electronics in Agriculture*. 187:106231.
- Zakir, E., Ogunlowo, Q. O., Akpenpuun, T. D., Na, W.-H., Adesanya, M. A., Rabiu, A., Adedeji, O. S., Kim, H. T., Lee, H.-W. 2022. Effect of thermal screen position on greenhouse microclimate and impact on crop growth and yield. *Nigerian Journal of Technological Development*. 19:417-32.

Zeng, S., Hu, H., Xu, L., Li, G. 2012. Nonlinear adaptive pid control for greenhouse environment based on rbf network. Sensors. 12:5328-48.

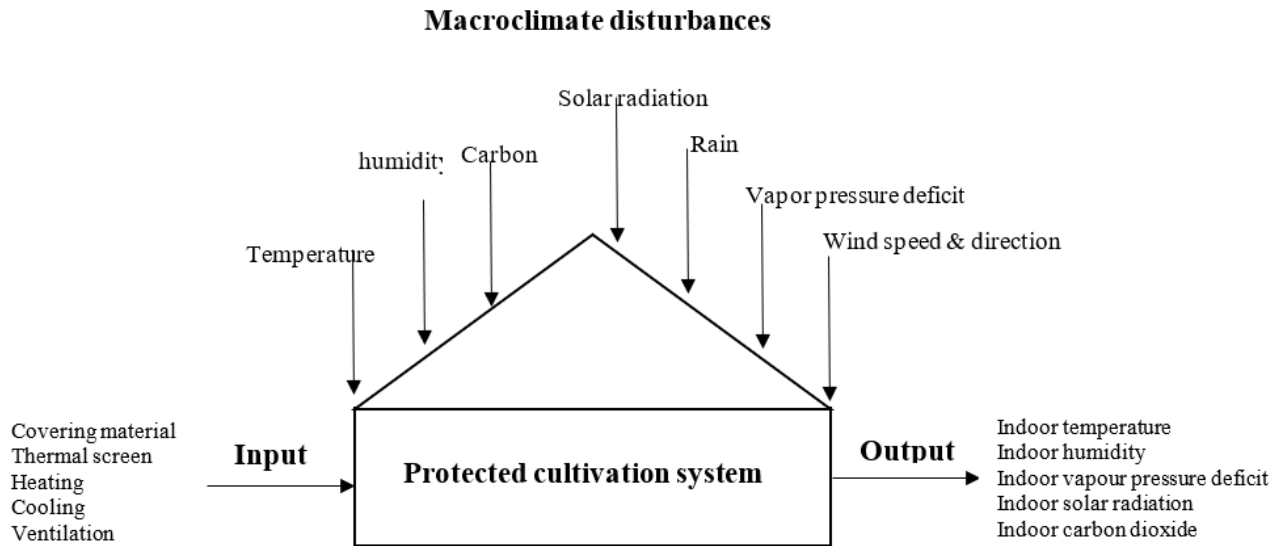


Figure 1. Greenhouse model.

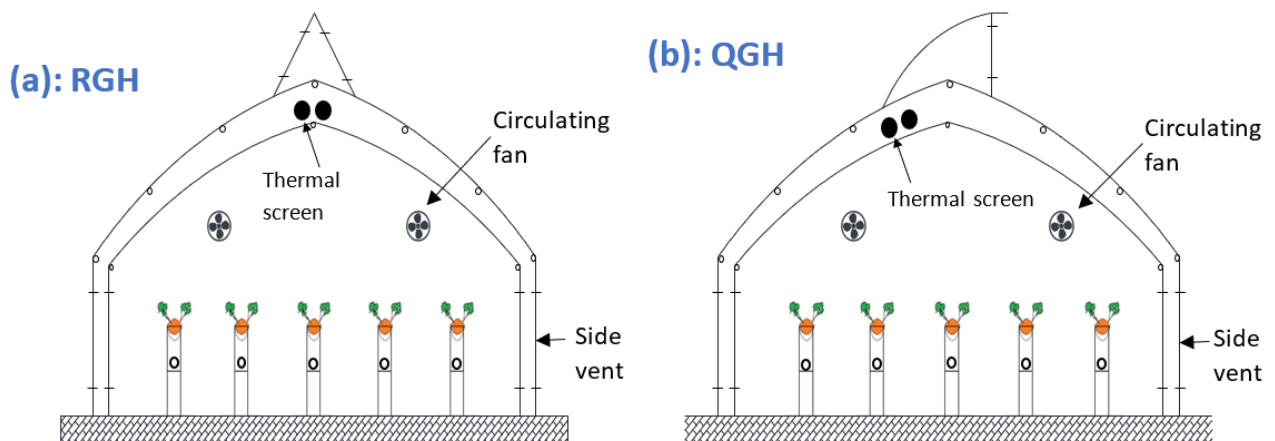


Figure 2. Thermal curtain positions.

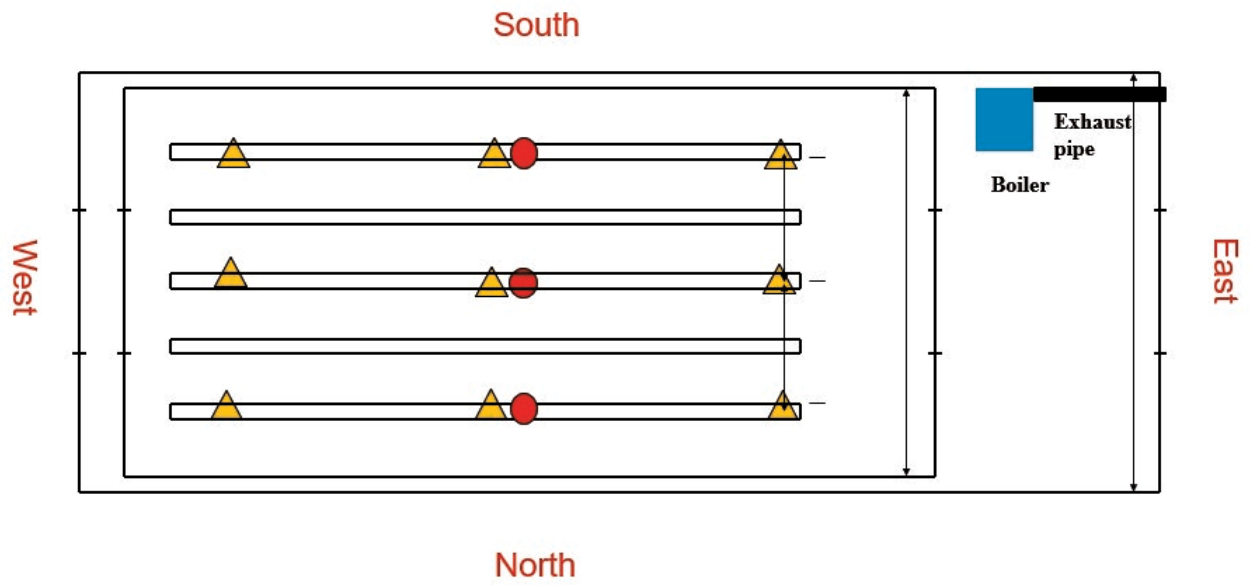


Figure 3. Sensor location in both greenhouses.

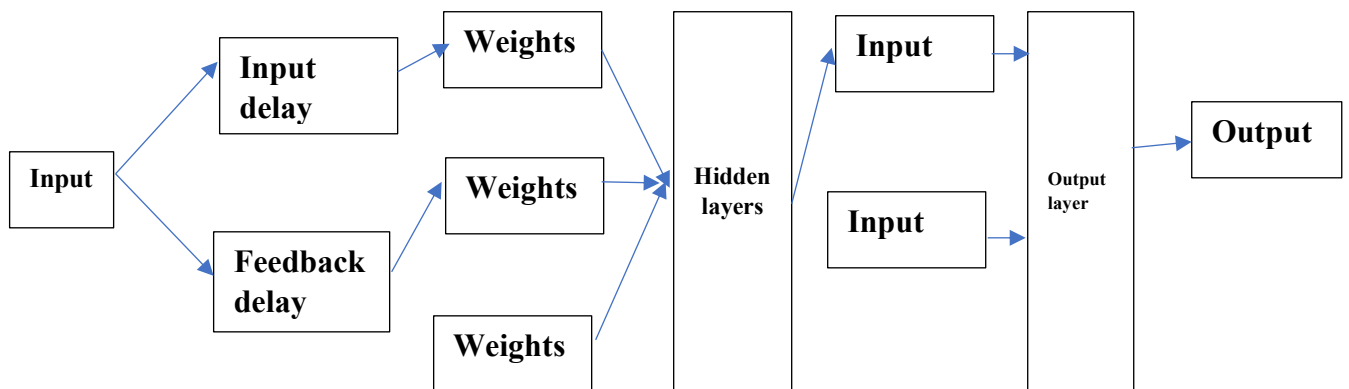


Figure 4. NARX architecture.

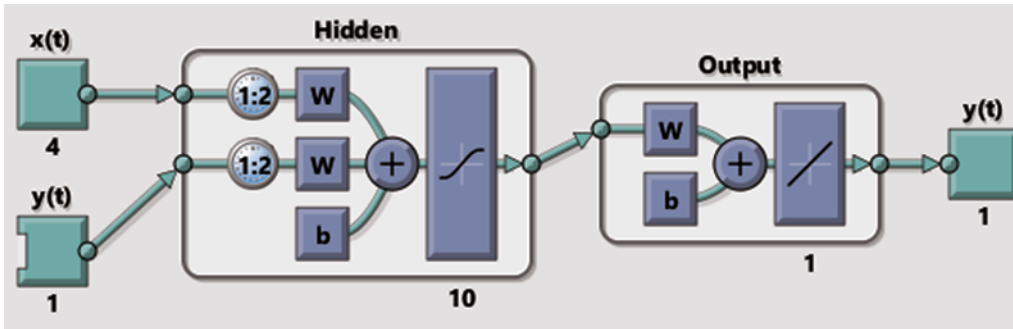


Figure 5. MATLAB NARX neural network diagram.

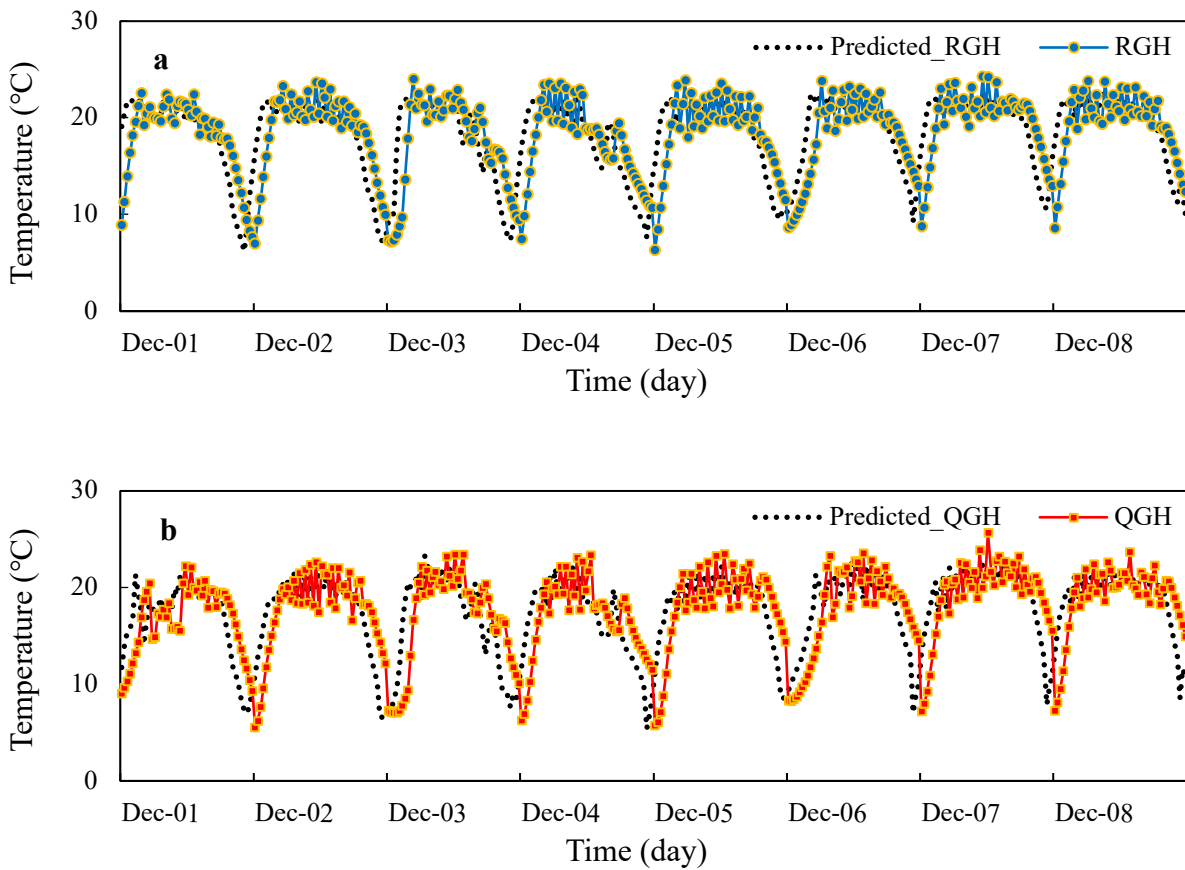


Figure 6. Predicted temperature in RGH and QGH.

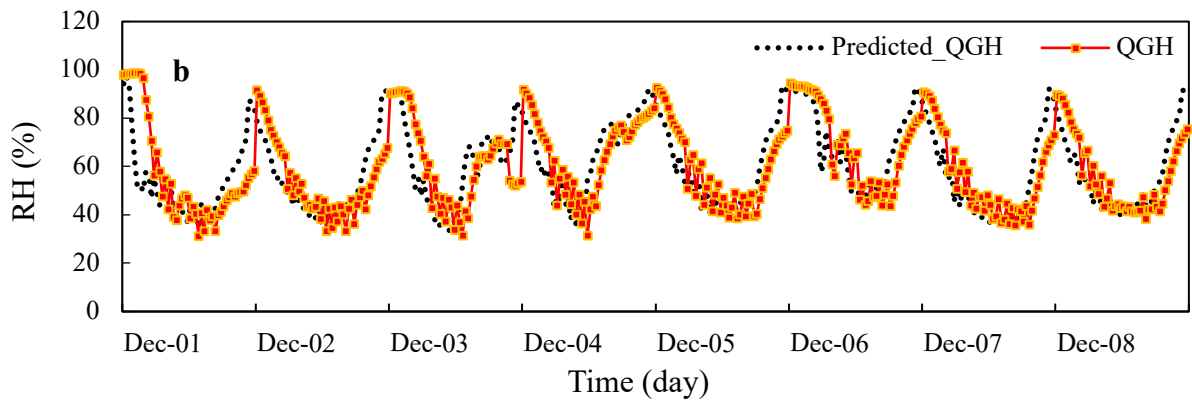
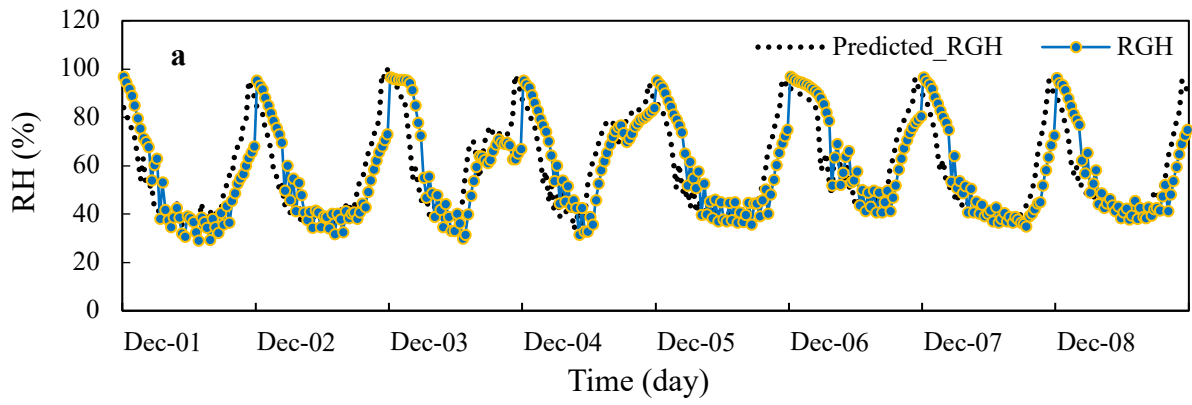


Figure 7. Predicted RH in RGH and QGH.

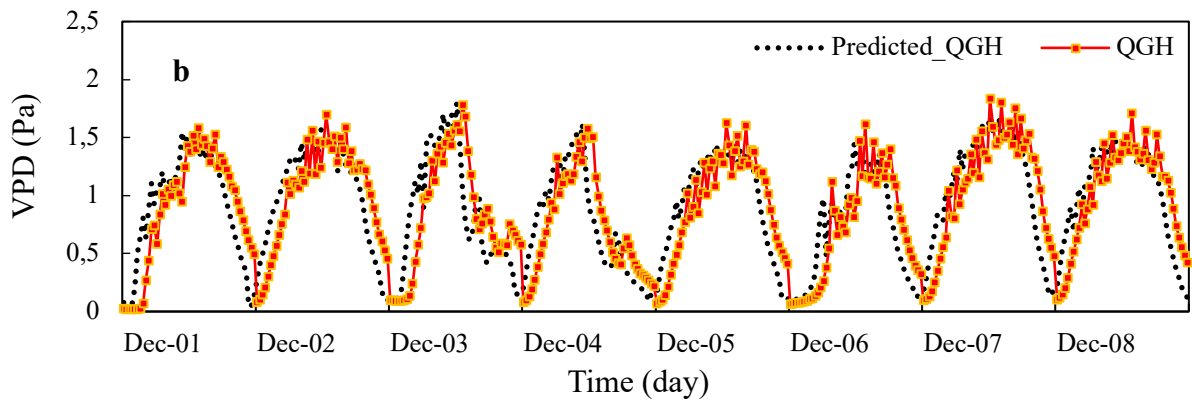
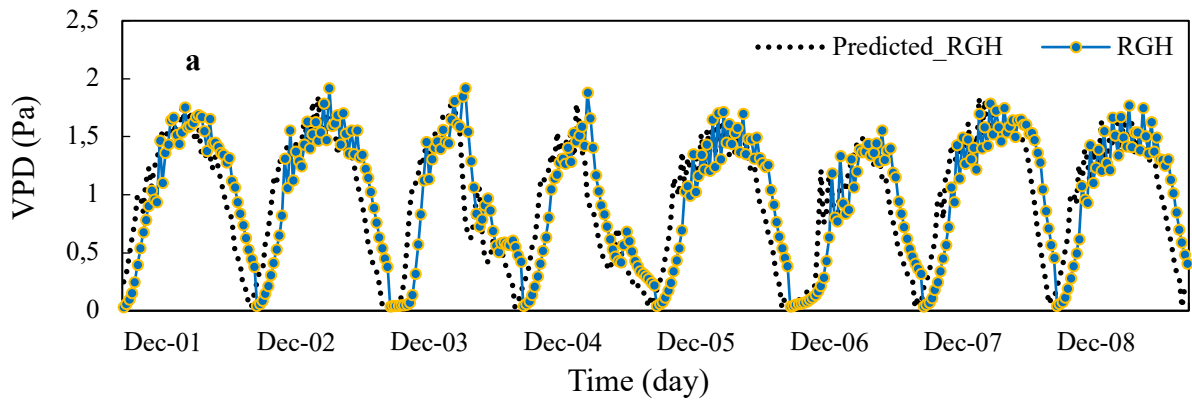


Figure 8. Predicted VPD in RGH and QGH.

Table 1. Descriptive statistics of microclimate parameters.

Parameter /Statistical tool		Mean	Standard error	Standard deviation	Sample variance	Range	Minimum	Maximum
Temperature	R	20.01	0.06	4.78	22.86	34.03	2.05	36.08
	Q	19.31	0.06	4.83	23.37	34.5	1.42	35.92
	Outside	9.16	0.09	7.54	56.83	41.77	-9.8	31.97
RH	R	50.32	0.27	22.01	484.28	84.33	13.77	98.11
	Q	52.36	0.26	21.06	443.32	84.31	14.36	98.67
	Outside	42.57	0.21	17.16	294.52	82.56	13.1	95.65
VPD	R	1.23	0.01	0.86	0.74	4.21	0.02	4.23
	Q	1.21	0.01	0.77	0.59	4.08	0.02	4.1
SR	R	254.64	1.83	150.67	22702.21	784.7	3.74	786.2
	Q	205.33	1.55	127.64	16291.06	535.7	2.13	536.82
	Outside	377.27	2.07	195.72	48728.31	977.2	5.54	982.80
irT	R	18.75	0.19	16.01	256.31	62.74	1.75	53.99
	Q	22.77	0.08	6.97	48.63	44.37	2.36	46.73
irRH	R	53.15	0.4	32.58	1061.38	90.69	5.47	96.16
	Q	44.49	0.27	22.06	486.68	86.69	10.01	96.71
Yield	R	6.33	0.02	1.58	2.51	6.69	3.82	13.51
	Q	7.72	0.03	1.92	3.70	11.77	4.68	16.44

Table 2. Model architecture and accuracy parameter for RGH.

Model	No. of hidden neurons: delays	Training: validation: testing	R ² , %			MSE			RMSE		
			Training	Validation	Testing	Training	Validation	Testing	Training	Validation	Testing
	10:02	70:15:15	97.6	97.2	96.8	9.66E-04	1.03E-04	1.24E-04	3.11E-02	1.01E-02	1.11E-02
T	10:03	70:15:15	97.6	97.1	97.3	9.20E-04	1.11E-04	1.07E-04	3.03E-02	1.05E-02	1.03E-02
	10:04	70:15:15	97.5	96.8	97.5	1.01E-04	1.17E-04	1.06E-04	1.00E-02	1.08E-02	1.03E-02
RH	10:02	70:15:15	97.2	97.8	97.6	3.77E-04	2.83E-04	3.37E-04	1.94E-02	1.68E-02	1.84E-02
	10:03	70:15:15	98.0	97.5	97.4	2.76E-04	3.24E-04	3.47E-04	1.66E-02	1.80E-02	1.86E-02
	10:04	70:15:15	98.1	97.4	97.3	2.31E-04	3.12E-04	3.95E-04	1.52E-02	1.77E-02	1.99E-02
	10:02	70:15:15	99.0	98.7	98.8	8.37E-04	1.12E-03	1.06E-03	2.89E-02	3.35E-02	3.26E-02
VPD	10:03	70:15:15	99.2	98.6	98.2	6.74E-04	1.14E-03	1.19E-03	2.60E-02	3.38E-02	3.45E-02
	10:04	70:15:15	99.1	98.7	98.6	7.60E-04	1.04E-03	1.13E-03	2.76E-02	3.22E-02	3.36E-02
Yield	10:02	70:15:15	99.9	99.9	99.9	4.27E-05	1.61E-05	1.91E-05	6.53E-03	4.01E-03	4.37E-03
	10:03	70:15:15	99.9	99.9	99.9	6.90E-05	8.13E-05	3.75E-05	8.31E-03	9.02E-03	6.12E-03
	10:04	70:15:15	99.9	99.9	99.9	5.83E-06	2.12E-05	1.20E-05	2.41E-03	4.60E-03	3.46E-03

Table 3. Model architecture and accuracy parameter for QGH.

Model	No. of hidden neurons: delays	Training: validation: testing	R ² , %			MSE			RMSE		
			Training	Validation	Testing	Training	Validation	Testing	Training	Validation	Testing
	10:02	70:15:15	97.2	97	97.4	1.04E-03	1.18E-03	1.10E-03	3.22E-02	3.44E-02	3.32E-02
T	10:03	70:15:15	97.3	97	97.3	1.03E-03	1.16E-03	1.11E-03	3.21E-02	3.41E-02	3.33E-02
	10:04	70:15:15	97.3	96.7	97.3	1.02E-03	1.14E-03	1.11E-03	3.19E-02	3.38E-02	3.33E-02
RH	10:02	70:15:15	97.3	97.6	97.5	3.28E-03	2.86E-03	3.21E-03	5.73E-02	5.35E-02	5.67E-02
	10:03	70:15:15	97.9	96.9	96.9	2.62E-03	3.79E-03	3.77E-03	5.12E-02	6.16E-02	6.14E-02
	10:04	70:15:15	97.9	97.4	97	3.01E-03	3.01E-03	3.70E-03	5.49E-02	5.49E-02	6.08E-02
	10:02	70:15:15	98.9	98.9	98.9	7.29E-04	8.09E-04	8.03E-04	2.70E-02	2.84E-02	2.83E-02
VPD	10:03	70:15:15	98.8	98.8	98.5	8.19E-04	8.73E-04	1.09E-03	2.86E-02	2.95E-02	3.30E-02
	10:04	70:15:15	98.8	98.4	98.7	8.66E-04	1.03E-03	9.42E-04	2.94E-02	3.21E-02	3.07E-02
	10:02	70:15:15	99.9	99.9	99.9	4.56E-05	1.83E-05	2.69E-05	6.75E-03	4.28E-03	5.19E-03
Yield	10:03	70:15:15	99.9	99.9	99.9	1.07E-05	1.99E-04	1.74E-05	3.27E-03	1.41E-02	4.17E-03
	10:04	70:15:15	99.9	99.9	99.9	9.08E-06	2.01E-05	2.74E-04	3.01E-03	4.48E-03	1.66E-02

Table 4. ANOVA of actual vs predicted data for RGH and QGH.

	RGH				QGH			
	T	RH	VPD	Yield	T	RH	VPD	Yield
F _{statistics}	9.26e-05	1.68e-04	0.13	0.05	0.08	0.02	0.04	0.01
P-value	0.99	0.99	0.72	0.82	0.77	0.89	0.84	0.90
F _{critical}	3.84	3.84	3.84	3.84	3.84	3.84	3.84	3.84

For T, RH and VPD: df1 = 1; df2 = 13526, For yield: df1 = 1; df2 = 11034

Table 5. Mean of parameters.

Parameter	RGH		QGH	
	Actual	Predicted	Actual	Predicted
Temperature, °C	20.01	20.01	19.31	19.29
RH, %	50.34	50.35	52.38	52.33
VPD, kPa	1.31	1.31	1.20	1.21
Yield, g	6.33	6.33	7.72	7.72

Table 6. Frequency distribution of VPD in RGH and QGH.

Description	VPD range	RGH		QGH	
		Actual	Predicted	Actual	Predicted
Optimal range	0.5–1.19	2490 (36.8%)	2445 (36.1%)	3045 (45%)	3114 (46%)
Outside optimal range	0.1–0.49/1.2–4.29	4274 (63.2%)	4319 (63.9%)	3719 (55%)	3650 (54%)